Electronic supplementary information (ESI)

Functional Double-Shelled Silicon Nanocrystals for Two-Photon Fluorescence Cell Imaging: Spectral Evolution and Tuning

Sourov Chandra, Batu Ghosh, Gregory Beaune, Usharani Nagarajan, Takao Yasui, Jin Nakamura, Tohru Tsuruoka, Dr. Yoshinobu Baba, Naoto Shirahata,* and Francoise M. Winnik*

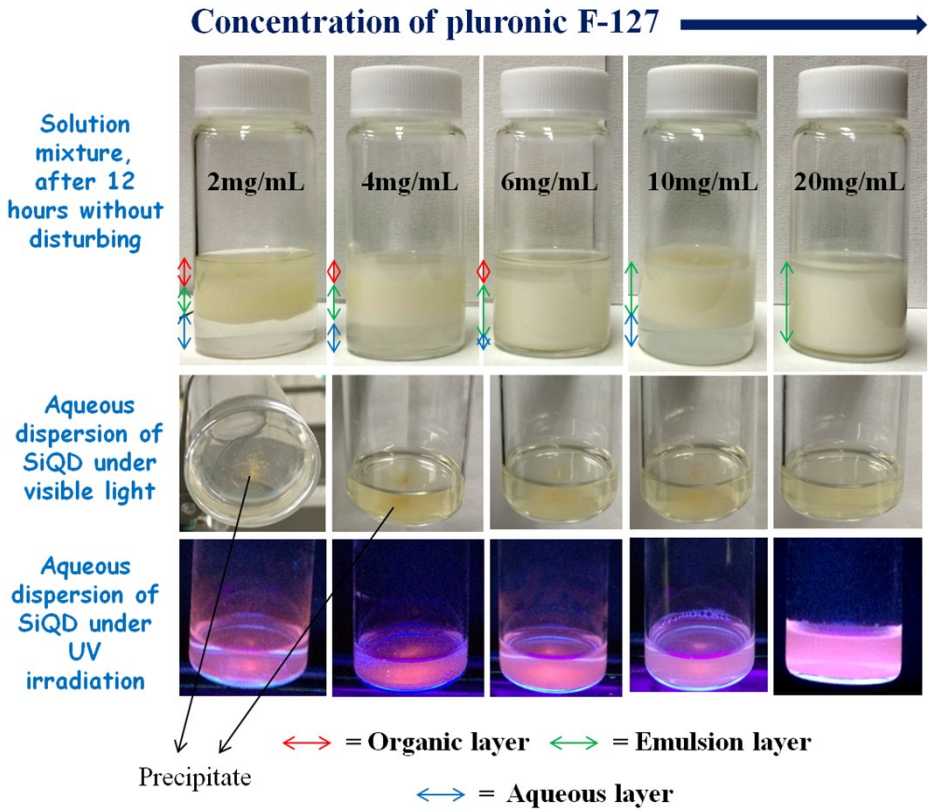

Fig. S1. Conversion of hydrophobic ncSi-OD to hydrophilic ncSi-OD/F127 by using different concentration of Pluronic F127 solution, where all other conditions were remaining unaltered. The upper panel showed the mixture of two phases and the stability of emulsion after 12 hours of mixing, whereas the middle and lower panels described the aqueous dispersion and agglomeration of ncSi-OD/F127 (SiQD marked in the figure) after evaporating the organic layer under visible light and UV-irradiation respectively.

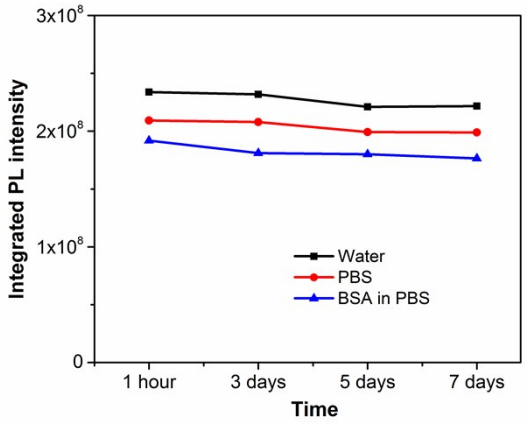

Fig. S2. Photostability of ncSi-OD/F127 NPs in non-luminescent water, PBS and BSA.

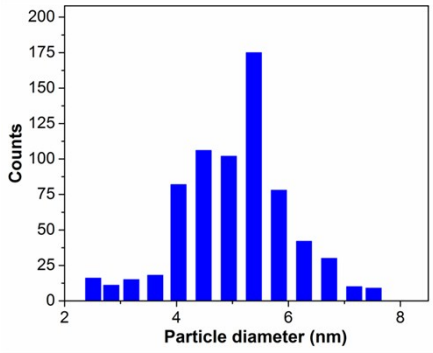

Fig. S3. Size distribution of the nanocrystals measured from HRTEM images of ncSi-OD sample.

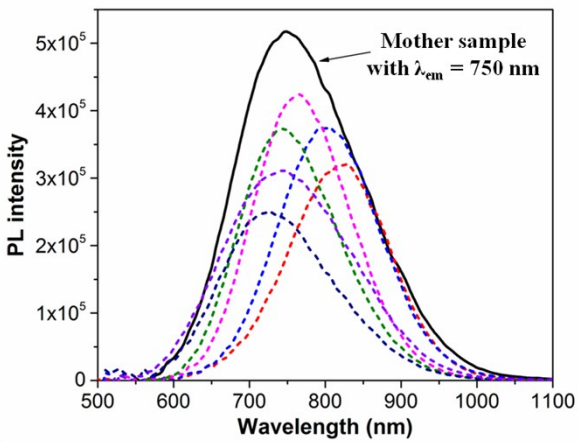

Fig. S4. PL spectrum decomposed into six different PL spectra (depicted with dotted lines) by separation with column chromatographic processes. The sample with a PL peak at 750 nm was used as a mother sample.

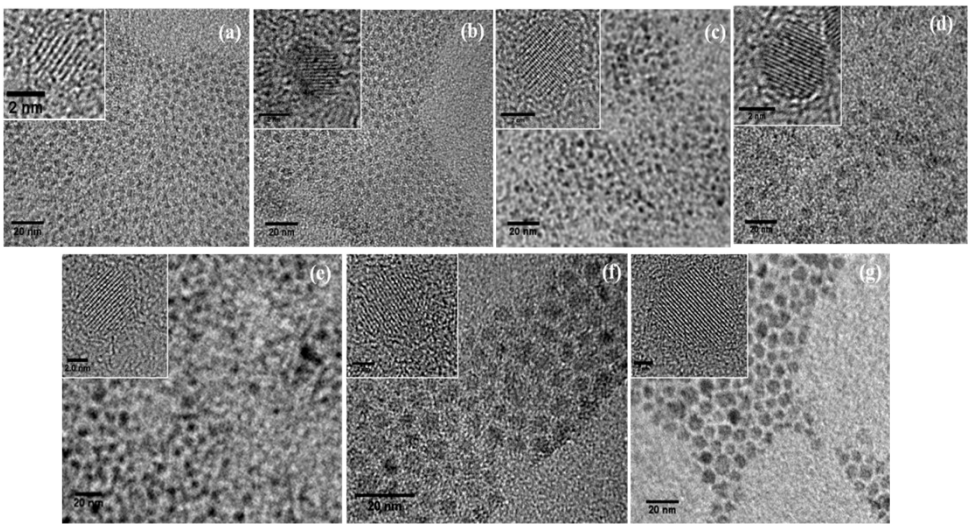

Fig. S5. HR-TEM images of ncSi-OD fractions obtained by the combined column separation technique. The samples are same to them listed in Table 1. The average diameters for each are (a) 2.5 nm, (b) 2.7 nm, (c) 3.2 nm, (d) 3.6 nm, (e) 4.6 nm, (f) 5.3 nm, and (g) 7.4 nm, respectively.

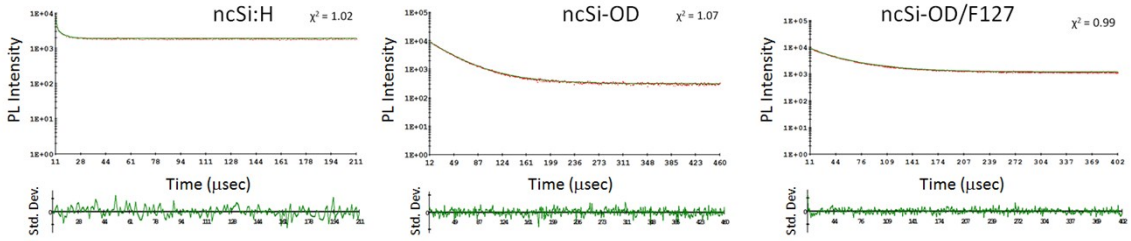

Fig. S6. Time-resolved PL decays of ncSi:H, ncSi-OD and ncSi-OD/F127 samples. Solid green lines are fits to each PL decay.

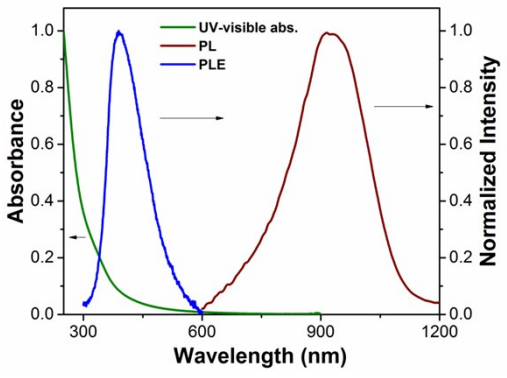

Fig. S7. Optical absorbance and emission spectra of ncSi-OD/F127 NPs in non-luminescent water.

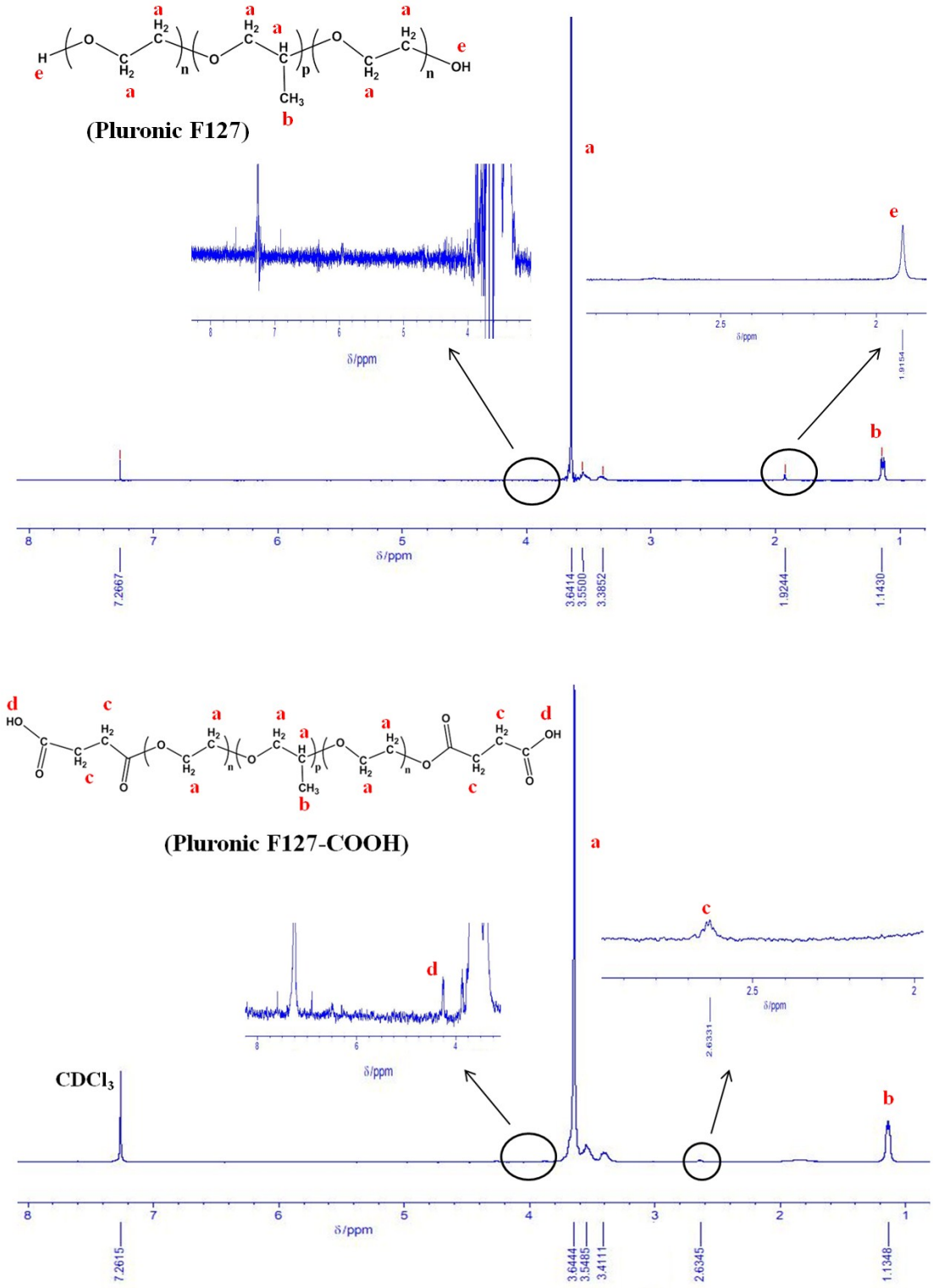

Fig. S8. ^{1}H-NMR spectra of (a) Pluronic F127 and (b) Pluronic F127-COOH